



**HAL**  
open science

# Solvatochromic behaviour of cyclic dithioether-functionalized triphenylamine ligands and their mechano-responsive Cu( i ) coordination polymers

Dilip Pandey, Gopal Singh, Shivendu Mishra, Lydie Viau, Michael Knorr, Abhinav Raghuvanshi

## ► To cite this version:

Dilip Pandey, Gopal Singh, Shivendu Mishra, Lydie Viau, Michael Knorr, et al.. Solvatochromic behaviour of cyclic dithioether-functionalized triphenylamine ligands and their mechano-responsive Cu( i ) coordination polymers. Dalton Transactions, 2023, 52, pp.14151-14159. 10.1039/D3DT02226A . hal-04225318

**HAL Id: hal-04225318**

**<https://hal.science/hal-04225318>**

Submitted on 2 Oct 2023

**HAL** is a multi-disciplinary open access archive for the deposit and dissemination of scientific research documents, whether they are published or not. The documents may come from teaching and research institutions in France or abroad, or from public or private research centers.

L'archive ouverte pluridisciplinaire **HAL**, est destinée au dépôt et à la diffusion de documents scientifiques de niveau recherche, publiés ou non, émanant des établissements d'enseignement et de recherche français ou étrangers, des laboratoires publics ou privés.

# Solvatochromic behavior of cyclic dithioether-functionalized triphenylamine ligands and their mechano-responsive Cu(I) coordination polymers

Dilip Pandey<sup>a</sup>, Gopal Singh<sup>a</sup>, Shivendu Mishra<sup>a</sup>, Lydie Viau<sup>b</sup>, Michael Knorr<sup>b</sup>, and Abhinav Raghuvanshi\*<sup>a</sup>

Email: [r.abhinav@iiti.ac.in](mailto:r.abhinav@iiti.ac.in)

<sup>a</sup>*Department of Chemistry, Indian Institute of Technology, Indore, MP, India, 452020.*

<sup>b</sup>*Université de Franche-Comté, UMR CNRS 6213, Institut UTINAM, 16 Route de Gray, F-25000 Besançon, France.*

## Abstract

Cu(I)-based coordination polymers (CPs) are known as efficient emissive materials providing an eco-friendly and cost-effective platform for the development of various functional materials and sensors. In addition to the nature of the metal center, organic ligands also play a crucial role in controlling the emissive properties of coordination polymers. Herein, we report on the synthesis of dithiane- and dithiolane-substituted triphenylamine ligands **L**<sub>1</sub> and **L**<sub>2</sub>. These ligands were found to be emissive both in the solid state and in solution. In addition, these ligands exhibit solvatochromic behavior due to the twisted intramolecular charge transfer (TICT) phenomenon. Next, coordination behavior of these ligands was explored with Cu(I)X salts (X = Br and Cl) and four new 1D coordination polymers [ $\{\text{Cu}(\mu_2\text{-X})_2\text{Cu}\}(\mu_2\text{-L})_n$ ], **CP1** (X = Br, L = **L**<sub>1</sub>), **CP2** (X = Cl, L = **L**<sub>1</sub>), **CP3** (X = Br, L = **L**<sub>2</sub>), and **CP4** (X = Cl, L = **L**<sub>2</sub>) were synthesized and crystallographically characterized. The emission behavior of all the CPs suggests ligand-centered transitions. On mechanical grinding, emission maxima ( $\lambda_{\text{em}}$ ) for **CP1** and **CP2** were blue-shifted, whereas for **CP3** and **CP4** red-shifts were observed. All CPs were found to emit at 448 nm with increased intensity after grinding. It is supposed that grinding is responsible for a change in the spatial arrangement (dihedral angles) of the phenyl groups of TPA, causing the observed emission shifts. Furthermore, the higher emission intensity after grinding suggest the occurrence of a similar phenomenon as an aggregation-induced quenching in these CPs.

## Introduction

External stimuli like light, pH, temperature, mechanical force and magnetic or electric fields can affect the luminescence behavior of various compounds.<sup>1-3</sup> Compounds with unique photoluminescent properties under different conditions are prominent materials for applications in sensing, detection, memory, display systems and others.<sup>4-6</sup> However, synthesizing materials that can respond in a controlled and desirable fashion under various external stimuli is challenging. Molecules with strong  $\pi$ - $\pi$  interaction in the aggregated state lead to quenching of emission called aggregation-caused quenching (ACQ), whereas enhanced emission in the aggregated state is known as aggregation-induced emission (AIE). In order to design stimuli-responsive fluorescent materials, mostly tetraphenylethene, triphenylamine, pyrene and anthracene derivatives have been employed as fundamental building blocks, which could control the emission via ACQ or AIE phenomenon. Among this group of fluorophores, the triphenylamine (TPA) unit stands out as an optoelectronically active motif capable of adopting a range of conformations. Because of the non-planar propeller-shaped arrangement of three aryl groups around the nitrogen atom TPA complexes usually show AIE. However, the occurrence of this phenomenon largely depends on the substituents present on the phenyl groups.<sup>7-13</sup> Several stimuli-responsive organic materials with TPA scaffold have been reported. However examples of metal-organic frameworks (MOFs) and coordination polymers (CPs), composed of TPA ligands showing any response in the presence of external stimuli are significantly less known.<sup>14-20</sup> Bu *et al.* have reported a Cd(II) coordination network using tris(4-(pyridin-4-yl)phenyl)amine ligand that exhibits thermo and mechano-luminescence properties due to change in dihedral angles between the three phenyl rings of the TPA core.<sup>20</sup> To the best of our knowledge, this is the only example of a CP or MOF, where the dihedral angles between the three phenyls of TPA affect the emission.

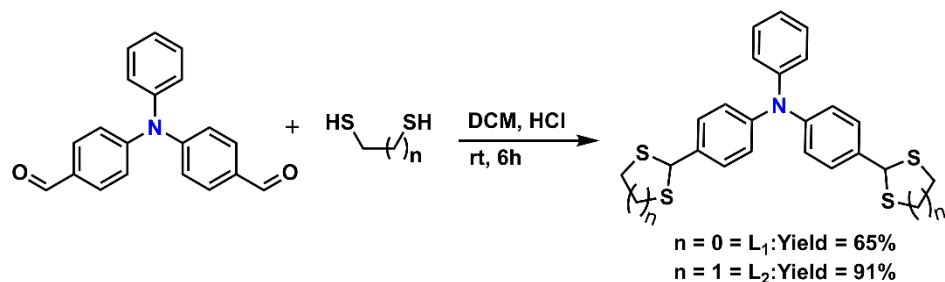
Copper(I) halides-based CPs are known as efficient emissive materials that offer a versatile platform for developing various stimuli-responsive, electrically-conductive sensors, and other functional materials.<sup>21-24</sup> Different  $\text{Cu}_n\text{X}_n$  cluster cores or secondary building units (SBUs) present in these CPs may control the dimensionality of the material and thereby affect their behavior and applications. These CPs may respond to various stimuli and show distinct changes in structural properties, mostly due to modification in Cu--Cu distance, cluster rearrangement,

and solid-to-solid phase transitions. These structural changes could also alter various moderate and weak inter- and intra-molecular interactions, which significantly affect the luminescent properties of the CPs.<sup>25-27</sup> The development of Copper(I)-based CPs using polydentate organosulfur ligands has gained significant interest lately as they offer a large structural diversity.<sup>28-34</sup> In the last few years, we have designed different cyclic dithioethers, which are easily accessible by condensing an aldehyde and dithiols  $\text{HS}(\text{CH}_2)_n\text{SH}$ , and used them as a connecting unit to construct various Copper(I) CPs.<sup>32-34</sup> It was observed that the architecture of these CPs and the nuclearity of the SBU's depend on several factors, such as the nature of ligands, the metal-to-ligand ratio and the reaction conditions like solvent, temperature, and pressure.

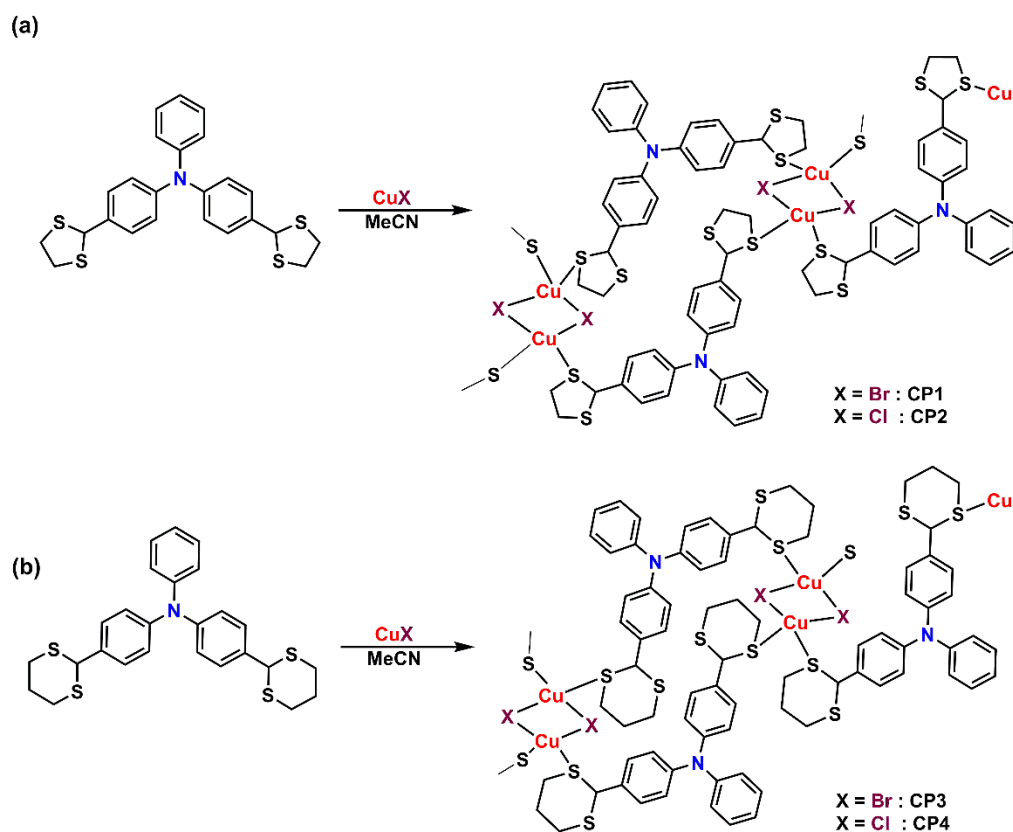
In this work, we have extended our study and substituted two out of three phenyl rings of triphenylamine unit with 1,3-dithiane or 1,2-dithiolane. The substitution on the third ring was avoided intentionally to allow the free movement of a phenyl group even after CP formation, as it can control the photophysical properties of the TPA unit. The coordination behavior of these substituted triphenylamine ligands with Cu(I) halides has been explored to obtain CPs incorporating  $\text{Cu}_2\text{X}_2$  SBUs. Since both organic and inorganic units possess unique photoluminescence properties, the objective was to study the combined effect on the resulting material's behavior.

## Results and Discussion

Ligands  $\text{L}_1$  and  $\text{L}_2$  were synthesized by reacting equimolar ratio of bis(4-formylphenyl)phenylamine with 1,2-ethanedithiol and 1,3-propanedithiol, respectively, in concentrated HCl at room temperature (Scheme 1). After work-up, both ligands were obtained as yellow solids in good yields (see ESI for experimental details). NMR spectroscopy and Mass spectrometry were used to characterize the resulting organosulfur compounds. In addition to the aromatic protons, the distinctive  $^1\text{H}$  NMR (Fig. S1 and S2 ESI) signals for the two methine protons at 5.63 and 5.13 ppm confirm the formation of the 1,3-dithiolane and 1,3-dithiane moieties on TPA. The structure of  $\text{L}_2$  was further authenticated by single-crystal X-ray analysis.



**Scheme 1** Synthesis of ligands **L<sub>1</sub>** and **L<sub>2</sub>**.



**Scheme 2** (a). Synthesis of **CP1** and **CP2** (b). Synthesis of **CP3** and **CP4**.

Subsequently, **CP1** and **CP2** of composition  $[\{\text{Cu}(\mu_2\text{-Br})_2\text{Cu}\}(\mu_2\text{-L}_1)]_n$ , and  $[\{\text{Cu}(\mu_2\text{-Cl})_2\text{Cu}\}(\mu_2\text{-L}_1)]_n$ , respectively, were synthesized by reacting ligand **L<sub>1</sub>** with CuBr and CuCl in acetonitrile (MeCN) solution at room temperature using a 1:2 molar ratio. The products were obtained as off-white solids with 83% yield for **CP1** and 79% yield for **CP2**. Similarly, **CP3** and **CP4** were synthesized by reacting **L<sub>2</sub>** with CuBr and CuCl in a 1:2 molar ratio. The final compounds were obtained as white microcrystalline powders with 69% and 52% yields for **CP3** and **CP4**, respectively (Scheme 2). Attempts to modify the dimensionality or SBUs of these CPs using

different ligands/metal ratios in different solvents and mixtures of solvents, including EtCN, CH<sub>3</sub>CN:DCM, CH<sub>3</sub>CN:MeOH, and CH<sub>3</sub>CN:DMF has not been conclusive and led to the same CPs, though a higher ratio of copper(I) salts provide better yield of CPs.

### Description of the crystal structures of L<sub>2</sub> and CP1-CP4

Crystals suitable for single crystal X-ray diffraction (SCXRD) analysis of L<sub>2</sub> were obtained by slow evaporation of a dichloromethane solution. L<sub>2</sub> crystallizes in the monoclinic P2<sub>1</sub>/c space group (Fig. 1 and Table S1(ESI)). The crystal structure suggests that the TPA unit is positioned in a propeller-like arrangement where the dihedral angles between the three phenyl planes are 89, 47 and 81°. Two of the three benzene rings are substituted with 1,3-dithiolane units at the *para*-position and both 1,3-dithiane units are arranged in a most stable chair conformation.

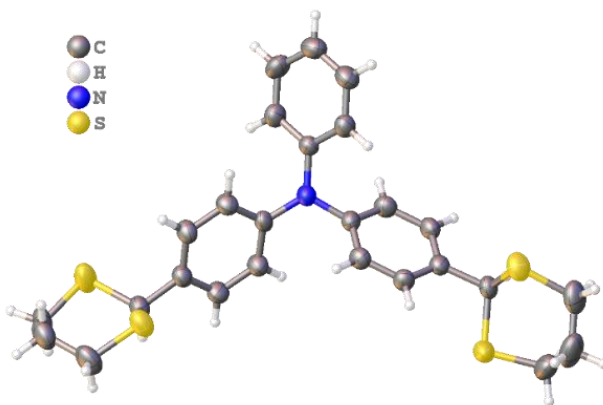


**Fig. 1** Molecular structure of L<sub>2</sub>.

All CPs were found insoluble in most of the common organic solvents but partially soluble in acetonitrile, propionitrile and DMF. In order to obtain suitable crystals for SCXRD analysis, the precipitates obtained after reactions were redissolved in boiling acetonitrile and left to evaporate partially at room temperature. Hexagon-shaped crystals of CP1, CP2, CP3 and plate-shaped crystals for CP4 were obtained after a few days. SCXRD data were collected at room temperature and crystallographic details are provided in Tables S1 and S2. The coordination polymers CP1 and CP2 crystallize in the triclinic  $P\bar{1}$  space group, whereas CP3 and CP4 crystallize in the monoclinic  $P2_1/n$  space group. Single crystal analysis of CP1-CP4 reveals the formation of 1D coordination polymers with centrosymmetric Cu( $\mu_2$ -X)<sub>2</sub>Cu (X = Br, Cl) rhomboid cores as SBUs confirming a 1:1 metal/ligand ratio (Fig. 2-5). Each Cu is coordinated

to two sulfur atoms stemming from different ligands and two bridging halide atoms. Out of the two sulfur atoms in the dithiolane/dithiane rings, only one coordinates with the metal. However, since the sulfur atoms of different rings coordinate to different Cu centers, ribbon-like 1D coordination polymers form in all cases.

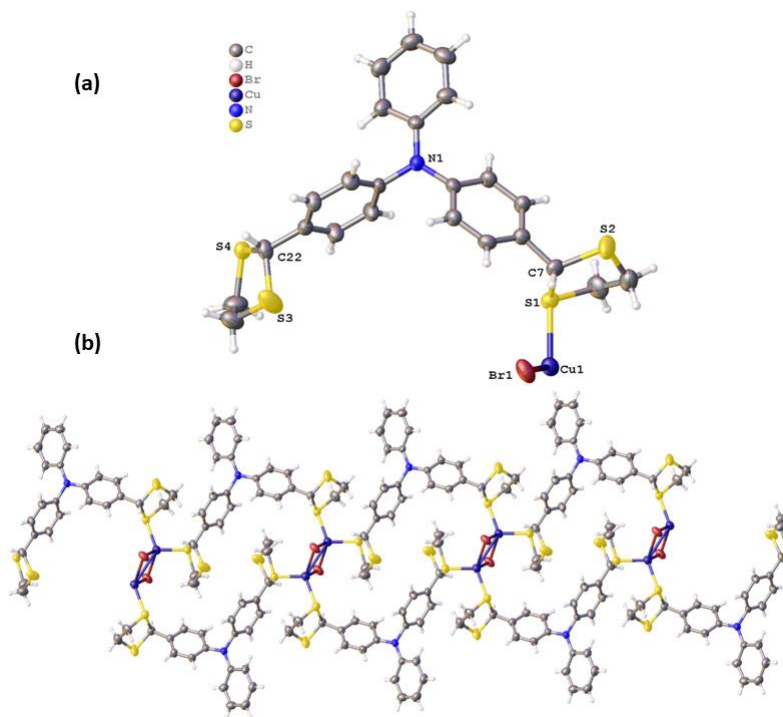


**Fig. 2** (a) individual motif of **CP1** (b) View of the 1D ribbon of  $[\{\text{Cu}(\mu_2\text{-Br})_2\text{Cu}\}(\mu_2\text{-L}_1)]_n$  (**CP1**) running along the  $a$  axis. Symmetry transformations used to generate equivalent atoms:  $^1\text{-X}, 1\text{-Y}, 1\text{-Z}$ ;  $^2\text{+X}, \text{+Y}, 1\text{+Z}$ ;  $^1\text{+X}, \text{+Y}, -1\text{+Z}$   $^1\text{+X}, \text{+Y}, -1\text{+Z}$   $^1\text{+X}, \text{+Y}, -1\text{+Z}$ ;  $^1\text{+X}, \text{+Y}, -1\text{+Z}$ .

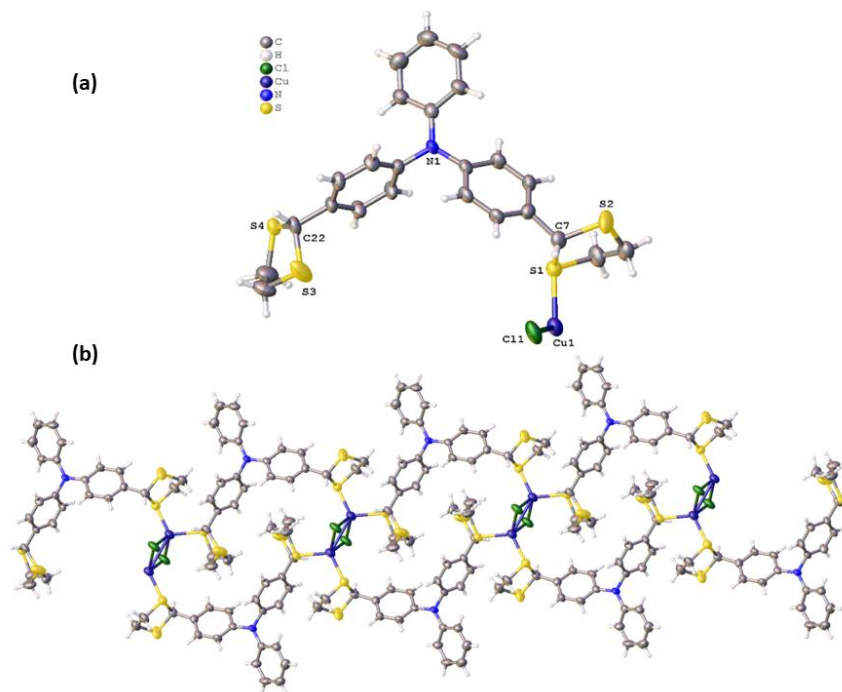


**Fig. 3** (a) individual motif of **CP2** (b) View of the 1D ribbon of  $[\{\text{Cu}(\mu_2\text{-Cl})_2\text{Cu}\}(\mu_2\text{-L}_1)]_n$  (**CP2**) running along the  $a$  axis. Symmetry transformations used to generate equivalent atoms:  $^1\text{-X}, 1\text{-Y}, 2\text{-Z}$ ;  $^2\text{+X}, \text{+Y}, 1\text{+Z}$ ;  $^1\text{-X}, 1\text{-Y}, 2\text{-Z}$ ;  $^2\text{+X}, \text{+Y}, 1\text{+Z}$ ;  $^3\text{+X}, \text{+Y}, -1\text{+Z}$ ;  $^1\text{+X}, \text{+Y}, -1\text{+Z}$ .

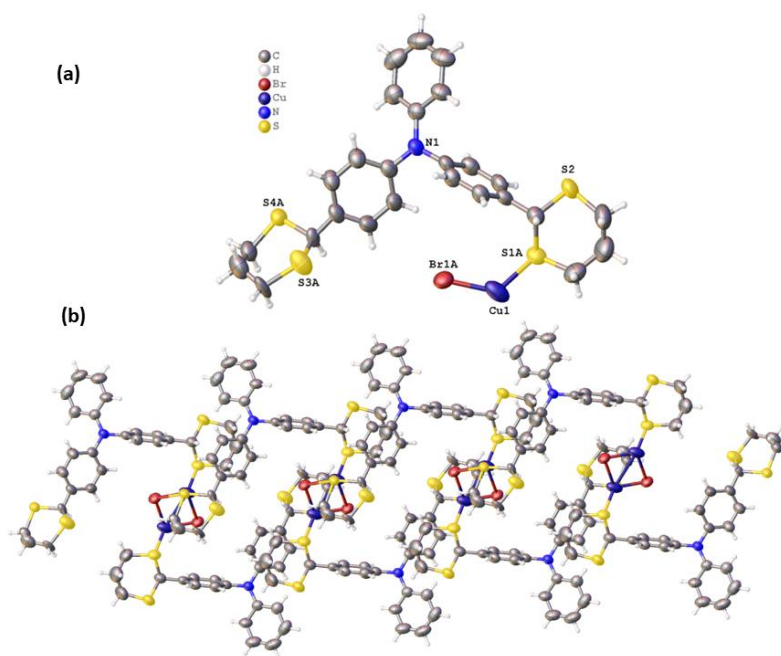


**Fig. 4 (a)** individual motif of **CP3** **(b)** View of the 1D ribbon of  $[\{\text{Cu}(\mu_2\text{-Br})_2\text{Cu}\}(\mu_2\text{-L}_2)]_n$  (**CP3**) running along the  $a$  axis. Symmetry transformations used to generate equivalent atoms:  $^11\text{-X},1\text{-Y},1\text{-Z}$ ;  $^21\text{+X},\text{+Y},\text{+Z}$ ;  $^11\text{-X},1\text{-Y},1\text{-Z}$ ;  $^21\text{+X},\text{+Y},\text{+Z}$ ;  $^3\text{-1+X},\text{+Y},\text{+Z}$ ;  $^1\text{-1+X},\text{+Y},\text{+Z}$ .

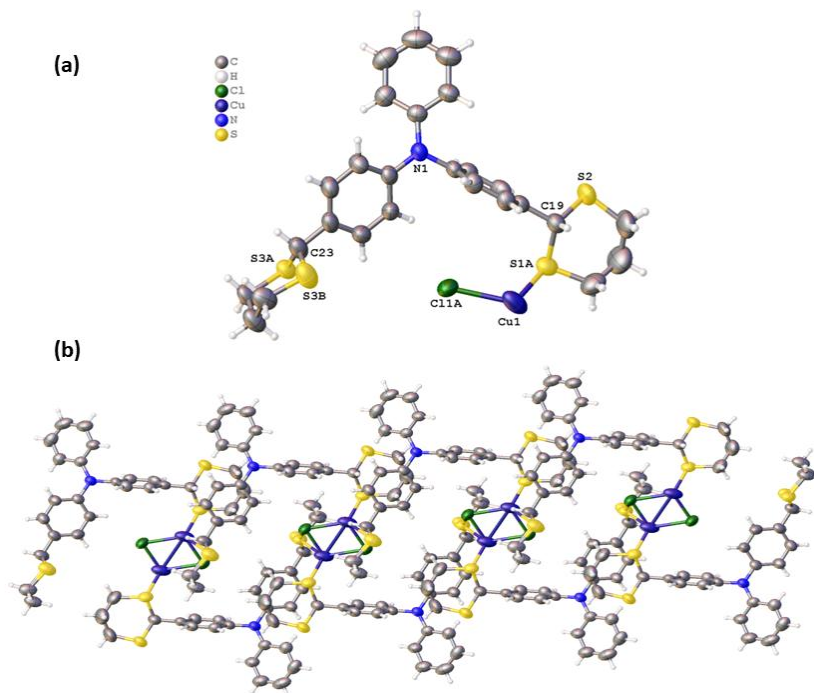


**Fig. 5 (a)** individual motif of **CP4** **(b)** View of the 1D ribbon of  $[\{\text{Cu}(\mu_2\text{-Cl})_2\text{Cu}\}(\mu_2\text{-L}_2)]_n$  (**CP4**) running along the  $a$  axis. Symmetry transformations used to generate equivalent atoms:  $^11\text{-X},1\text{-Y},1\text{-Z}$ ;  $^21\text{+X},\text{+Y},\text{+Z}$ ;  $^11\text{-X},1\text{-Y},1\text{-Z}$ ;  $^21\text{+X},\text{+Y},\text{+Z}$ ;  $^3\text{-1+X},\text{+Y},\text{+Z}$ ;  $^1\text{-1+X},\text{+Y},\text{+Z}$ .

The geometric parameters for these CPs agree well with the values found in the similar-reported Cu(I) halide CPs having S-coordinated  $\text{Cu}_2\text{X}_2$  units.<sup>31-34</sup> However, there is a significant deviation in structure for **CP1** to **CP4**. A comparison of the more relevant average bond lengths and average bond angles of all four CPs are summarized in Table 1 and Table 2. **CP2** and **CP4** incorporating a  $\text{Cu}(\mu_2\text{-Cl})_2\text{Cu}$  unit have similar  $\text{Cu}\cdots\text{Cu}$  distances ( $\sim 2.92$  Å) but **CP1** and **CP3** having  $\text{Cu}(\mu_2\text{-Br})_2\text{Cu}$  unit feature slightly different  $\text{Cu}\cdots\text{Cu}$  distances (2.97 Å for **CP1** and 2.91 Å for **CP3**). Since these  $\text{Cu}\cdots\text{Cu}$  separations are clearly beyond the van der Waals radii of two copper atoms (2.8 Å), one may exclude any cuprophilic bonding interaction.<sup>35</sup> Examples of other 1D materials featuring  $\text{Cu}(\mu_2\text{-X})_2\text{Cu}$  SBUs with  $\text{Cu}\cdots\text{Cu}$  contacts in a similar range are  $[\{\text{Cu}(\mu_2\text{-$

Br)<sub>2</sub>Cu} {μ<sub>2</sub>-PhS(CH<sub>2</sub>)<sub>3</sub>SPh}<sub>2</sub>]<sub>n</sub><sup>36</sup> [ {Cu(μ<sub>2</sub>-Br)<sub>2</sub>Cu} (bis(phenylthio)methane)<sub>2</sub>]<sub>n</sub><sup>37</sup> and [ {Cu(μ<sub>2</sub>-Cl)<sub>2</sub>Cu} (μ<sub>2</sub>-2-methyl-1,3-dithiane)<sub>2</sub>]<sub>n</sub>.<sup>38</sup> Because of different Cu···Cu distance, the Cu—Br—Cu angle is more acute in **CP3** (71.67°) in comparison to **CP1** (74.18°). The average Cu—Br distance is 2.46 Å and the average Cu—Cl distance is 2.35 Å, which is similar to the previously reported examples.<sup>35-38</sup> In addition, CPs formed by 1,2-ditholane have shorter Cu—S bond lengths compared to CPs formed by 1,3-dithiane ((~ 2.29 vs. ~ 2.36 Å).). The average S—Cu—X angle is close to 107° for **CP1** and **CP3** (X = Br), whereas this angle is close to 113° for **CP2** and **CP4** (X = Cl). In all four CPs, the coordination leads to the formation of 32-membered macrocycles with a maximum distance of approximately 12.5 Å between the centroids of the phenyl groups of different TPA units in a cycle (Fig. S7-S10 ESI). From the crystal structures, it can be seen that the planes of the phenyl rings are oriented at different angles with respect to each other (Table 5). Further, the packing arrangement of these CPs indicates multiple intermolecular C—H···π interactions between the 1D chains and some intramolecular C—H···π interactions ranging from 2.75 to 3.15 Å (Fig. S3-S6 ESI).

**Table 1.** Selected bond lengths (Å) for **CP1-CP4**.

Compounds	Average Cu—Cu	Average Cu—X	Average Cu—S
<b>CP1</b>	2.97	2.46	2.29
<b>CP2</b>	2.92	2.35	2.28
<b>CP3</b>	2.91	2.47	2.36
<b>CP4</b>	2.92	2.35	2.35

**Table 2.** Selected bond angles (°) for **CP1-CP4**.

Compounds	Average Cu—X—Cu	Average S—Cu—X	Average S—Cu—S
<b>CP1</b>	74.18	107.31	110.40
<b>CP2</b>	76.65	113.21	111.49
<b>CP3</b>	71.67	107.66	111.62

Powder X-ray diffraction (PXRD) studies were performed at room temperature and a comparison of experimental PXRD data with simulated ones obtained from single-crystal X-ray analysis confirms the phase purity of the samples (Fig. S12.1 and S12.2 ESI). All four CPs were found to be stable at room temperature in open vials for several months. Moreover, thermogravimetric analysis (TGA) was performed on all the compounds, confirming their stability up to 200 °C (Fig. S14 ESI).

### **Photophysical studies and solvatochromic behavior of ligands**

TPA-based luminogens are known to be quite sensitive in response to solvent polarity and show exceptional solvatochromic properties.<sup>39-41</sup> We recorded the luminescence of the synthesized ligands in different solvents and found that both ligands **L**<sub>1</sub> and **L**<sub>2</sub> are solvato-fluorochromic (Fig. 6). Both ligands show similar emission behavior in different solvents. The excitation maxima (365 nm) were constant across the solvent types, while the emission maxima were red-shifted when increasing the polarity of the solvent (the parameters for solvent polarity expressed as  $E_T(30)$  values are reported in Table 3).<sup>42</sup> The highest energy emission bands are observed at 415 (**L**<sub>1</sub>) and 418 nm (**L**<sub>2</sub>) in hexane, while the lowest energy band at 524 and 526 nm appear in DMSO for **L**<sub>1</sub> and **L**<sub>2</sub>, respectively.

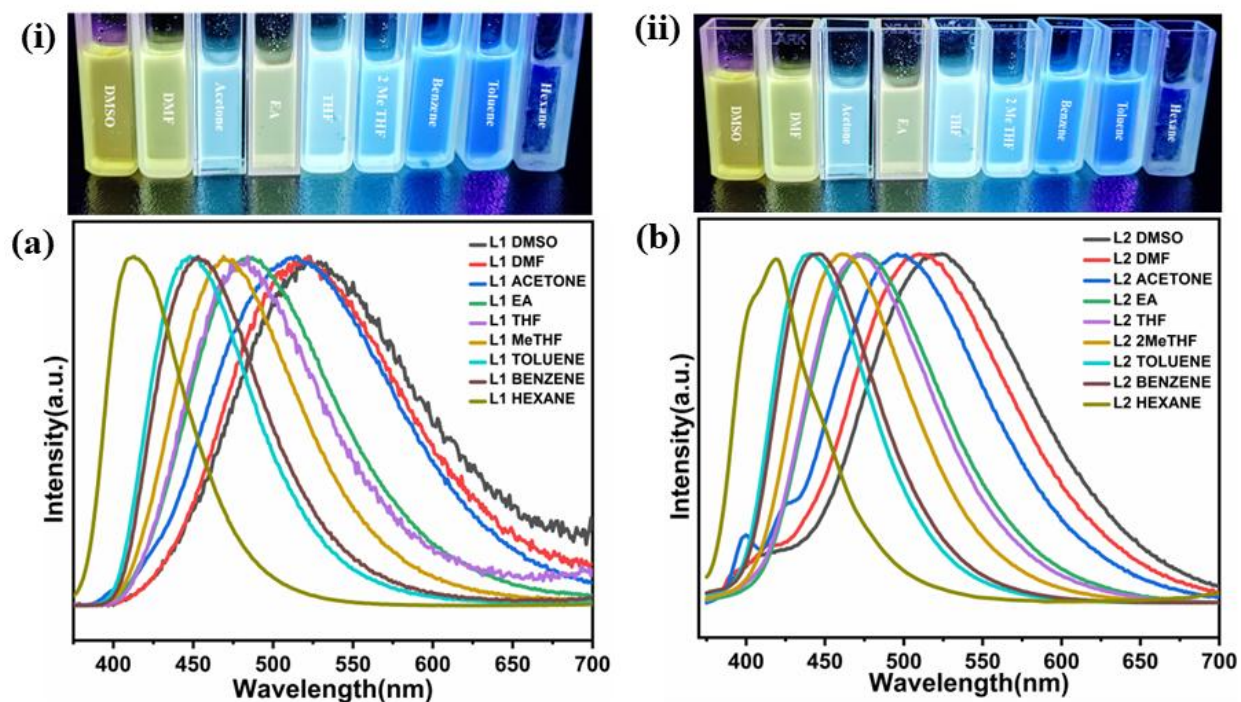


**Fig. 6** (i) Photographs taken under UV lamp ( $\sim 365$  nm) for  $L_1$ , (ii) photographs taken under UV lamp ( $\sim 365$  nm) for  $L_2$ , (a) emission spectra of ligand  $L_1$  in different organic solvents, (b) emission spectra of ligand  $L_2$  in different organic solvents.

Similar solvatochromic effects in triphenylamine derivatives have already been observed and were explained by the involvement of a higher energy locally excited (LE) state that favors a coplanar conformation and a low energy twisted state.<sup>43-46</sup> The excited luminogens planar conformation can be stabilized in nonpolar solvents, producing a high energy and short-wavelength emission of the LE state. The structure of luminogen rotates intramolecularly in polar solvents, changing its state from LE to twisted intramolecular charge transfer (TICT) and accelerating the intramolecular transfer of electrons from donor to acceptor moieties. We propose a similar TICT phenomenon with our ligands that results in a red-shifted emission of ligands in polar solvents.

**Table 3.** Excitation  $\lambda_{\text{abs}}$  and emission  $\lambda_{\text{em}}$  maxima for  $L_1$  and  $L_2$  in different solvents

Solvents	$E_T(30) /$ $\text{kcal mol}^{-1}$	$\lambda_{\text{abs}} /$ $\text{nm}$	$\lambda_{\text{em}} /$ $\text{nm (L}_1\text{)}$	$\lambda_{\text{em}} /$ $\text{nm (L}_2\text{)}$
DMSO	45.1	365	524	526

<b>DMF</b>	41.8	365	519	512
<b>Acetone</b>	42.2	365	513	499
<b>Ethyl Acetate</b>	38.0	365	484	475
<b>THF</b>	37.4	365	480	473
<b>2-Me-THF</b>	36.5	365	469	461
<b>Benzene</b>	34.3	365	454	445
<b>Toluene</b>	33.9	365	450	442
<b>Hexane</b>	32.4	365	415	418

**E<sub>T</sub>(30)**: Parameter of solvent polarity  $\lambda_{\text{abs}}$ - wavelength at electronic absorption maximum  $\lambda_{\text{em}}$ : wavelength at emission maximum.

To get an insight into the luminescence behavior, *ab initio* calculations based on Density-Function Theory (DFT) at the B3LPY/6-31+G(d,p) level have been performed with the Gaussian 09 program on **L**<sub>2</sub>.<sup>47</sup> It was found that the excited state LUMO density was more heavily weighted toward the substituted phenyl moiety of TPA, while the ground state HOMO density was found to be at 1,3-dithiolan-2-yl (Fig. 7). Moreover, the unsubstituted phenyl and substituted phenyl moieties are substantially twisted in the excited states. This observation is similar to previously reported systems and suggests TICT in the excited states of ligands.<sup>43-46</sup>

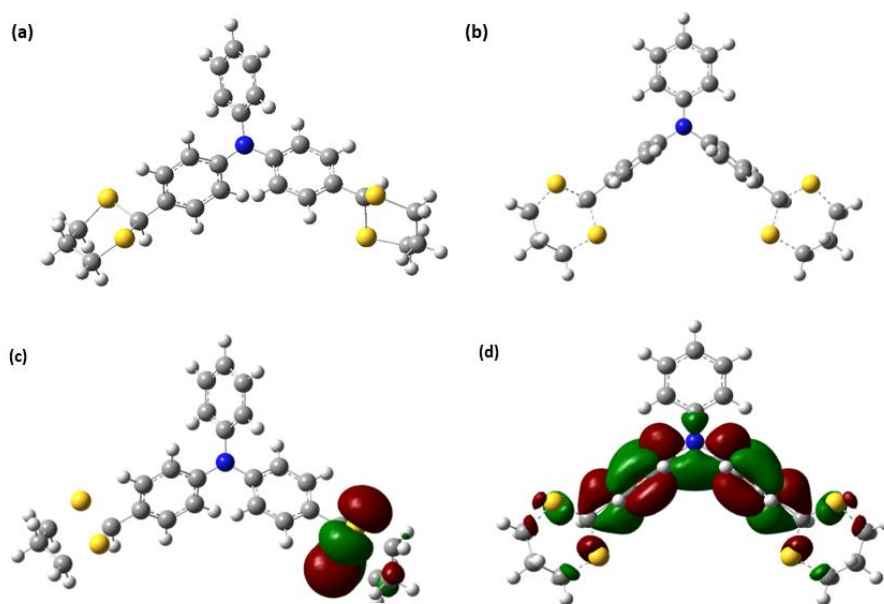


**Fig. 7** Calculated molecular structures of **L<sub>2</sub>** by DFT (a) Ground state (b) Excited state (c) HOMO in the ground state (d) LUMO excited state.

### Photophysical studies and mechanochromic behaviour of CPs

Solid-state photoluminescent properties were recorded for all the synthesized CPs at room temperature (Figure 10). All the compounds are off-white solids under ambient light and show cyan-blue luminescence under UV light (~365 nm) (Fig. 8). It was observed that upon excitation at 382 nm, **CP1** and **CP2** emit at lower energy (452 and 463 nm) compared to **CP3** and **CP4** (426 & 427 nm). In order to understand the origin of the emission, luminescence spectra of **L<sub>1</sub>** and **L<sub>2</sub>** have also been recorded in the solid state. The emission maxima for **L<sub>1</sub>** and **L<sub>2</sub>** were observed at 448 and 427 nm (Fig. S11 ESI), which is close to the emission of respective CPs and suggests that the ligand-centered transitions are responsible for the emission in the CPs.

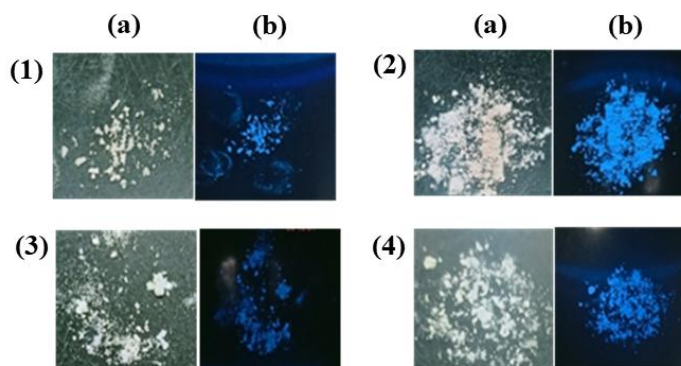


**Fig. 8** Photoluminescent images of (1). **CP1** (2). **CP2** (3). **CP3** and (4). **CP4** ; (a): under ambient light, (b): under UV lamp (~365 nm).

We observed that all CPs show interesting mechanochromic behavior. Mechanical grinding of **CP1** and **CP2** causes a small blue shift in emission from 452 and 463 nm to 448 nm with a significant increase in the intensity (Fig. 9a, b). Contrary to this, **CP3** and **CP4** display a red shift in emission from 426 and 427 nm to 448 nm with increased intensity (Fig. 9c, d). Interestingly, after grinding, emission maxima for all the CPs were found at the same wavelength (Fig. 10 and Table 4). Note that a similar occurrence of mechanochromism phenomenon was not observed with the ligands.

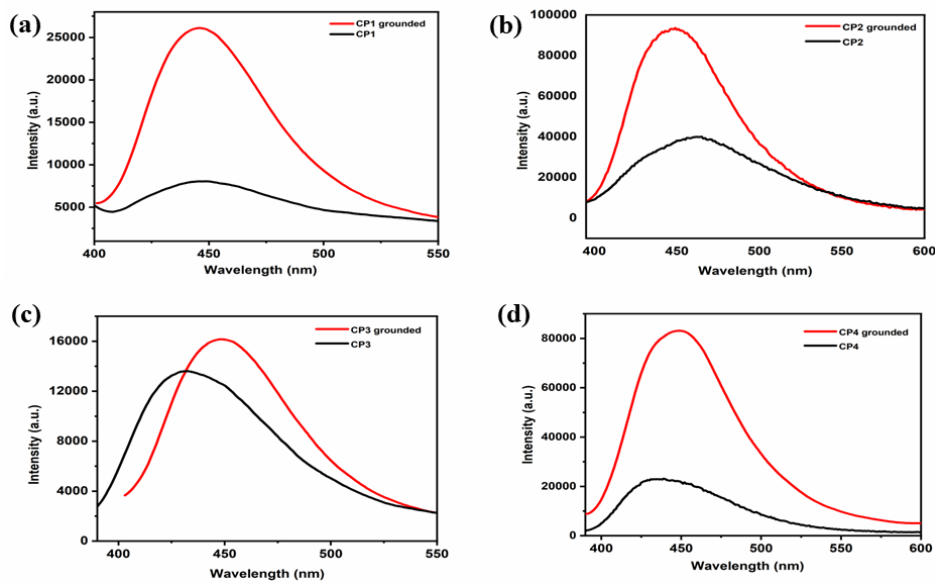


**Fig. 9** Emission spectra of CPs with the grounded sample at an excitation wavelength of 382 nm  
(a) CP1 (b) CP2 (c) CP3 (d) CP4.

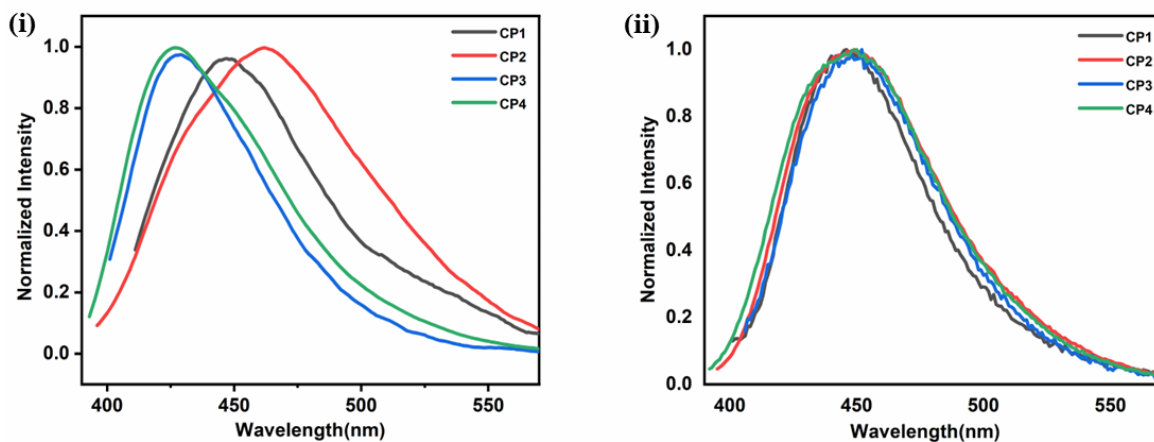


**Fig. 10** (i) Normalized emission spectra of pristine CP1, CP2, CP3 and CP4, (ii) luminescence emission spectra of grounded CP1, CP2, CP3 and CP4.

**Table 4.** Change in emission  $\lambda_{em}$  of all CPs after grinding.

Compounds	$\lambda_{abs}$ (nm)	$\lambda_{em}$ (nm)	
		Pristine solid	Grounded
CP1	382	452	448
CP2	382	463	448

<b>CP3</b>	382	426	448
<b>CP4</b>	382	427	448

It has been reported that the dihedral angles between the planes of phenyl groups of TPA affect the emission behaviour of TPA-derived compounds.<sup>7, 20</sup> To gain further insight, we checked the crystal structure and found that **CP1** and **CP2** have similar dihedral angles between the planes of phenyl groups of TPA which is significantly different from **CP3** and **CP4** (Table 5). In the case of **CP1** and **CP2**, the dihedral angles between the plane of the phenyl ring of TPA are approximately 85°, 86° and 56° and while in **CP3** and **CP4**, these angles are approximately 82°, 88° and 44°. The unusual blue shift and red shift observed after grinding could be attributed to the conformational twisting of the aromatic rings. Probably after grinding the samples, the angles between the plane of the phenyl rings orient somewhere in between and are similar in all CPs, resulting in the same emission.

**Table 5.** The dihedral angle between the planes of different phenyl rings (**Ph<sub>S</sub>** – substituted phenyl and **Ph<sub>f</sub>** – free phenyl).

<b>Compounds</b>	<b>Ph<sub>S</sub> – Ph<sub>f</sub></b>	<b>Ph<sub>S</sub> – Ph<sub>S</sub></b>	<b>Ph<sub>S</sub> – Ph<sub>f</sub></b>
<b>CP1</b>	85.45	86.6	55.95
<b>CP2</b>	84.06	85.15	57.14
<b>CP3</b>	81.88	88.35	44.82
<b>CP4</b>	81.57	88.34	44.28

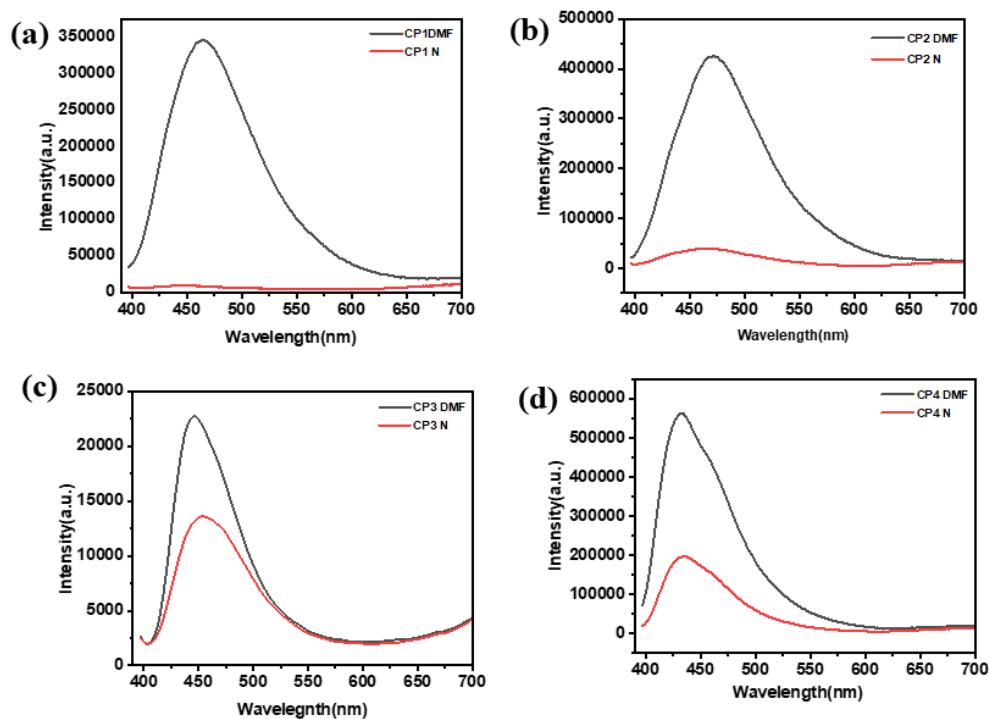


**Fig. 11** Emission spectra of CPs in the presence of DMF solvent at an excitation wavelength of 382 nm.

In addition to the shifting, also an increased emission intensity was observed after grinding the CPs. We further checked the geometric structures and packing arrangements of the CPs. No  $\pi$ - $\pi$  interactions were observed between the phenyl group of the ligands in the crystal structures. However, as shown in Fig. S5-S8 (ESI), multiple C-H $\cdots\pi$  inter- and intra-molecular interactions, with distances ranging from 2.75 to 3.15 Å, were found between different H-atoms and  $\pi$ -cloud of the phenyl rings of TPA units. These multiple C-H $\cdots\pi$  interactions probably contribute to an increase of intermolecular non-radiative transitions, causing an effect similar to ACQ.<sup>19</sup> On grinding, these C-H $\cdots\pi$  interactions could be partially removed; as a result, intramolecular radiative transitions are enhanced, thereby increasing emission intensity.<sup>2, 48-50</sup> To approve this hypothesis, we have recorded the PXRD of all four CPs after grinding. By comparison with the data of pristine solid, a loss in crystallinity is suggested to some extent (Fig. S13 ESI). Further, the presence of solvent vapors could eliminate or decrease the weak inter- and intramolecular interactions in a similar way. In order to verify this, we have recorded the emission of CPs in the presence of solvent vapors. When the solid product was exposed to DMF vapors for 12 hours, a significant increase in the emission intensity was observed, similar to that observed after

mechanical grinding (Fig. 11), confirming a phenomenon similar to the ACQ in all four CPs presented in this work.

## Conclusions

This study investigates the structural characteristics and photophysical behaviour of the triphenylamine-based ligands **L**<sub>1</sub> and **L**<sub>2</sub>, and their Cu(I) coordination polymers. It was observed that both ligands **L**<sub>1</sub> and **L**<sub>2</sub> display solvato-fluorochromic properties due to the TICT phenomenon. With a Cu<sub>2</sub>X<sub>2</sub> (X = Br and Cl) rhomboid cluster as SBU, four 1-D polymeric chains were synthesized, which exhibit mechanochromic properties as well. Grinding the CPs results in two phenomena: (i) a shift in emission maxima and (ii) an increase in emission intensity. The former effect results from the change in the angle between the free and coordinated phenyl groups that leads to the same  $\lambda_{em}$  for all the CPs. The later effect was observed due to the relaxation of C–H··· $\pi$  interactions leading to enhanced intensity. This was further confirmed by emission intensity enhancement in the presence of solvent vapors.

In conclusion, the variation in the ligand backbone around cyclic dithioethers and their coordination product could lead to the development of functional materials for different applications. We are currently investigating the coordination behavior of TPA ligand with dithioether substitution on all three phenyls in anticipation of getting a luminescent MOF-like structure for sensing applications.

## Experimental:

### Synthesis of CP1, CP2, CP3, and CP4:

General procedure: In a 50 mL Schlenk tube, ligand **L**<sub>1</sub> or **L**<sub>2</sub> (1 eq.) was dissolved in acetonitrile, and CuX (X = Br and Cl) (2 eq.) was separately dissolved in acetonitrile under N<sub>2</sub>. A few drops of methanol were also added to the CuX solution to avoid Cu(I) oxidation. After that, CuX solution was added to the ligand solution and the reaction mixture was stirred for 6 h at room temperature. After completion of the reaction, formation of off-white coloured products were observed, which were washed with 5 mL DCM (2-3 times). The yields of the final compounds, **CP1**, **CP2**, **CP3**, and **CP4** were 83%, 79%, 69%, and 52%, respectively.

**Acknowledgment:** We are grateful to IIT Indore for the financial support. We thank SIC IIT Indore and DST-FIST 500 MHz NMR facility by the Department of Chemistry, IIT Indore for providing characterization facilities.

### Conflict of Interest.

There are no conflicts to declare.

Electronic supplementary information (ESI) available: detailed experimental synthesis, information for SCXRD, Summary of X-ray data collection and refinement for all structures studied, PXRD patterns of **CP1–CP4** and TGA analysis of **CP1–CP4**. CCDC 2242123, 2242124, 2242127, 2242128 and 2242129.

### References

1. K. Nakamura, K. Kanazawa and N. Kobayashi, *J. Photochem. Photobiol. C*, 2022, 100486.
2. P. Xue, J. Ding, P. Wang and R. Lu, *J. Mater. Chem. C*, 2016, **4**, 6688-6706.
3. B. Li, H.-T. Fan, S.-Q. Zang, H.-Y. Li and L.-Y. Wang, *Coord. Chem. Rev.*, 2018, **377**, 307-329.
4. V. Stavila, A. A. Talin and M. D. Allendorf, *Chem. Soc. Rev.*, 2014, **43**, 5994-6010.
5. J.-Q. Liu, Z.-D. Luo, Y. Pan, A. K. Singh, M. Trivedi and A. Kumar, *Coord. Chem. Rev.*, 2020, **406**, 213145-213190.
6. G. Givaja, P. Amo-Ochoa, C. J. Gómez-García and F. Zamora, *Chem. Soc. Rev.*, 2012, **41**, 115-147.
7. P. Gayathri, M. Pannipara, A. G. Al-Sehemi and S. P. Anthony, *New J. Chem.*, 2020, **44**, 8680-8696.
8. Q.-F. Liang, H.-W. Zheng, D.-D. Yang and X.-J. Zheng, *CrystEngComm*, 2022, **24**, 543-551.
9. Z. Ning, Z. Chen, Q. Zhang, Y. Yan, S. Qian, Y. Cao and H. Tian, *Adv. Funct. Mater.*, 2007, **17**, 3799-3807.
10. Y. Zhang, Y.-Q. Feng, J.-H. Wang, G. Han, M.-Y. Li, Y. Xiao, and Z.-D. Feng, *RSC Adv.*, 2017, **7**, 35672-35680.
11. W. Hu, W. Yang, T. Gong, W. Zhou and Y. Zhang, *CrystEngComm*, 2019, **21**, 6630-6640.
12. J. B. Birks, *Photophysics of Aromatic Molecules*, Wiley, London, 1970.
13. B. Huang, D. Jiang, Y. Feng, W.-C. Chen, Y. Zhang, C. Cao, D. Shen, Y. Ji, C. Wang and C.-S. Lee, *J. Mater. Chem. C*, 2019, **7**, 9808-9812.
14. L.-X. Hu, M. Gao, T. Wen, Y. Kang and S. Chen, *Inorg. Chem.*, 2017, **56**, 6507-6511.

15. X.-S. Du, B.-J. Yan, J.-Y. Wang, X.-J. Xi, Z.-Y. Wang and S.-Q. Zang, *Chem. Commun.*, 2018, **54**, 5361-5364.
16. S. S. Liu, S. Yuan, T. P. Hu and D. Sun, *Z Anorg Allg Chem* 2014, **640**, 2030-2034.
17. Z. Shi, Z. Pan, H. Jia, S. Chen, L. Qin and H. Zheng, *Cryst. Growth Des.*, 2016, **16**, 2747-2755.
18. C. Hua, P. Turner and D. M. D'Alessandro, *Dalton Trans.*, 2015, **44**, 15297-15303.
19. B. Wu, Z. Guo, G. Li, J. Zhao, Y. Liu, J. Wang, H. Wang and X. Yan, *Chem. Commun.*, 2021, **57**, 11056-11059.
20. Z. Q. Yao, J. Xu, B. Zou, Z. Hu, K. Wang, Y. J. Yuan, Y. P. Chen, R. Feng, J. B. Xiong and J. Hao, *Angew. Chem. Int. Ed.*, 2019, **58**, 5614-5618.
21. E. Cariati, E. Lucenti, C. Botta, U. Giovanella, D. Marinotto and S. Righetto, *Coord. Chem. Rev.*, 2016, **306**, 566-614.
22. A. Schlachter, K. Tanner and P. D. Harvey, *Coord. Chem. Rev.*, 2021, **448**, 214176-214211.
23. K. Tsuge, Y. Chishina, H. Hashiguchi, Y. Sasaki, M. Kato, S. Ishizaka and N. Kitamura, *Coord. Chem. Rev.*, 2016, **306**, 636-651.
24. Y. Fang, W. Liu, S. J. Teat, G. Dey, Z. Shen, L. An, L. Wang, D. M. O'Carroll and J. Li, *Advanced Functional Materials*, 2017, **27**, 1603444-160353.
25. K. A. Vinogradova, N. A. Shekhovtsov, A. S. Berezin, T. S. Sukhikh, M. I. Rogovoy, A. V. Artem'ev and M. B. Bushuev, *Dalton Trans.*, 2021, **50**, 9317-9330.
26. T. Wen, D.-X. Zhang, J. Liu, R. Lin and J. Zhang, *Chem. Commun.*, 2013, **49**, 5660-5662.
27. A. Schlachter and P. D. Harvey, *J. Mater. Chem. C*, 2021, **9**, 6648-6685.
28. D. Li, W.-J. Shi and L. Hou, *Inorg. Chem.*, 2005, **44**, 3907-3913.
29. T. H. Kim, Y. W. Shin, J. H. Jung, J. S. Kim and J. Kim, *Angew. Chem. Int. Ed.*, 2008, **47**, 685-688.
30. J. Conesa-Egea, F. Zamora and P. Amo-Ochoa, *Coord. Chem. Rev.*, 2019, **381**, 65-78.
31. P. D. Harvey and M. Knorr, *J. Inorg. Organomet. Polym. Mater.*, 2016, **26**, 1174-1197.
32. A. Raghuvanshi, N. J. Dargallay, M. Knorr, L. Viau, L. Knauer and C. Strohmann, *J. Inorg. Organomet. Polym. Mater.*, 2017, **27**, 1501-1513.
33. A. Raghuvanshi, M. Knorr, L. Knauer, C. Strohmann, S. Boullanger, V. Moutarlier and L. Viau, *Inorg. Chem.*, 2019, **58**, 5753-5775.
34. L. Viau, M. Knorr, L. Knauer, L. Brieger and C. Strohmann, *Dalton Trans.*, 2022, **51**, 7581-7606.
35. N. S. Harisomayajula, S. Makovetskyi and Y. C. Tsai, *Chem. Eur. J.*, 2019, **25**, 8936-8954.
36. M. Knorr, F. Guyon, A. Khatyr, C. Strohmann, M. Allain, S. M. Aly, A. Lapprand, D. Fortin and P. D. Harvey, *Inorg. Chem.*, 2012, **51**, 9917-9934.
37. M. Knorr, A. Khatyr, A. Dini Aleo, A. El Yaagoubi, C. Strohmann, M. M. Kubicki, Y. Rousselin, S. M. Aly, D. Fortin and A. Lapprand, *Cryst. Growth Des.*, 2014, **14**, 5373-5387.
38. A. Raghuvanshi, M. Knorr, L. Knauer, C. Strohmann, S. Boullanger, V. Moutarlier and L. Viau, *Inorg. Chem.*, 2019, **58**, 5753-5775.
39. Z. R. Grabowski, K. Rotkiewicz and W. Rettig, *Chem. Rev.*, 2003, **103**, 3899-4032.

40. J. Zhang, B. He, Y. Hu, P. Alam, H. Zhang, J. W. Lam and B. Z. Tang, *Adv. Mater.*, 2021, **33**, 2008071-2008101.
41. Y. Yu, R. Zhao, H. Liu, S. Zhang, C. Zhou, Y. Gao, W. Li and B. Yang, *Dyes Pigm.*, 2020, **180**, 108511-108517
42. J. P. Cerón- Carrasco, D. Jacquemin, C. Laurence, A. Planchat, C. Reichardt and K. Sraïdi, *J. Phys. Org. Chem.*, 2014, **27**, 512-518.
43. K. Mizuguchi, H. Kageyama and H. Nakano, *Mater. Lett.*, 2011, **65**, 2658-2661.
44. R. Hu, E. Lager, A. Aguilar-Aguilar, J. Liu, J. W. Lam, H. H. Sung, I. D. Williams, Y. Zhong, K. S. Wong and E. Pena-Cabrera, *J. Phys. Chem. C*, 2009, **113**, 15845-15853.
45. S. Sasaki, G. P. Drummen and G.-i. Konishi, *J. Mater. Chem. C*, 2016, **4**, 2731-2743.
46. C. Wang, Q. Qiao, W. Chi, J. Chen, W. Liu, D. Tan, S. McKechnie, D. Lyu, X. F. Jiang, W. Zhou, N. Xu, Q. Zhang, Z. Xu and X. Liu, *Angew. Chem. Int. Ed.*, 2020, **59**, 10160-10172.
47. M. Frisch, G. Trucks, H. Schlegel, G. Scuseria, M. Robb, J. Cheeseman, G. Scalmani, V. Barone, B. Mennucci and G. Petersson, *Inc., Wallingford, CT*, 2009.
48. C. Y. Chan, J. W. Lam, Z. Zhao, S. Chen, P. Lu, H. H. Sung, H. S. Kwok, Y. Ma, I. D. Williams and B. Z. Tang, *J. Mater. Chem. C*, 2014, **2**, 4320-4327.
49. Y. Sun, Z. Lei and H. Ma, *J. Mater. Chem. C*, 2022, **10**, 14834-14867.
50. X. Zhang, Z. Chi, Y. Zhang, S. Liu and J. Xu, *J. Mater. Chem. C*, 2013, **1**, 3376-3390.